

# A New Paradigm in Chaotic Ray Scattering

G. Castaldi,<sup>1</sup> V. Fiumara,<sup>2</sup> V. Galdi,<sup>1</sup> V. Pierro,<sup>1</sup> and I.M. Pinto<sup>1</sup>

<sup>1</sup>*Wavesgroup, University of Sannio at Benevento, Italy*

<sup>2</sup>*Wavesgroup, D.I.<sup>3</sup>E., University of Salerno, Italy*

(Dated: March 30, 2022)

We introduce a new paradigm of (electromagnetic) 2D ray-chaos, featuring both guided and scattered rays in a dielectric layer with exponentially tapered refraction index backed by an undulated conductive surface, and illustrate its relevant features. Numerical simulations of the corresponding full-wave solution indicate that the system complies with Berry's conjecture in the asymptotic short wavelength limit.

PACS numbers: 05.45.Mt, 42.15.Dp, 42.25.Fx

## I. INTRODUCTION

Ray-chaos (exponential separation of nearby-originating rays, due to the geometrical features of the reflecting boundaries, and/or the refractive properties of the medium) is a lively subject, as witnessed by an increasing number of topical papers.

Well known paradigms of two-dimensional (henceforth 2D) ray-chaos include the Sinai [1] and Bunimovic [2] billiards (*internal* boundary value problems) and the  $n$ -disk ( $n \geq 3$ ) pinball-scatterer (*external* boundary value problem) [3]. These systems have been extensively studied both theoretically [4], in view of their relevance in the context of quantum chaology [5], and experimentally (see e.g. [6], and [7]), thanks to the formal equivalence between the 2D Schrödinger equation for a point particle in an infinite-wall potential, and the 2D (scalar) Helmholtz equation with perfectly conducting boundaries of Electromagnetics, which makes an experimental approach based on microwave measurements viable.

In this paper we introduce and analyze a new intriguing paradigm in ray-chaotic electromagnetic (henceforth EM) boundary-value problems. In its simplest (2D) form, the problem's geometry is sketched in fig. 1, and consists of a dielectric layer with exponentially tapered refraction index matched at  $z = 0$  to the outer vacuum (viz.,  $n(0) = 1$ ), and backed by a smooth perfectly-conducting periodic (undulated) surface  $z = \zeta(x)$ .

This geometry bears several elements of novelty. It is, perhaps, the simplest (2D) internal/external electromagnetic ray-chaotic boundary value problem featuring *both* guided *and* scattered rays at the same time. It also includes a (linear, isotropic, time-invariant, non-dispersive) dielectric layer as a basic ingredient at variance of billiards and pinballs, which are pure perfect-conductor-and-vacuum problems.

The 2D ray trajectories bear some similarity to the space-time ones of the well known (one-dimensional) Fermi-Pustil'nikov billiard [8], In this analogy, the gradient of the refractive-index plays the role of gravity, bending the ray-paths downward in the dielectric layer, while the undulated surface plays the role of the vibrating table, changing the slope of the ray at each bounce.

## II. RAY TRACING

The system in Fig. 1 can be parametrized in terms of the dimensionless variables  $n_f = n(-h)$ ,  $a/h$ ,  $\Delta/a$ . In this section we illustrate the main relevant results of straightforward ray-tracing simulations run for the geometry of Fig. 1, with  $a/h = 1$  and  $\Delta/a = 2\pi/5$ .

In Fig. 2 three examples are shown of (multi-hop) ray-paths originating from rays with close-by incidence points ( $\Delta x \sim 10^{-3}a$ ) and the same incidence angle ( $\theta_i = \pi/12$ ). In all three cases, a rapidly *increasing* ray separation is observed, resulting into completely different exit-angles. It will be shown soon that the ray separation increases exponentially in time, as the rays bounce back and forth through the dielectric layer.

In Fig. 3 the exit-angle is shown vs. the (scaled) incidence point position  $\bar{x} = x/a$ ,  $a$  being the spatial period of the undulated surface, for a fixed incidence angle  $\theta_i = \pi/12$ , and a few representative values of  $n_f$ . Intervals of distinctly *irregular* behaviour are observed. The measure of the set of incidence points corresponding to regular behaviour is seen to depend on the value of  $n_f$ , and shrinks to zero as  $n_f$  is increased. On the other hand, at fixed  $n_f$ , the measure of the set of incidence points corresponding to regular behaviour is found to be essentially *independent* of the incidence angle, as exemplified in Fig. 4, where  $n_f = 15$  and  $\theta_i = k\pi/12$ ,  $k = 1, 3, 5$ .

Closer investigation reveals that smaller and smaller intervals of regular behaviour are hidden within *arbitrarily small* intervals of  $\bar{x}$ , as shown in Fig. 5 for  $\theta_i = \pi/12$ .

As anticipated, in the *irregular* regime, the separation between neighbouring incident rays increases *exponentially*, as the rays bounce back and forth through the dielectric layer. This is shown in Fig. 6, where the logarithm of the ray-separation (in units of its initial value) is displayed as a function of time (sec) for  $n_f = 15$ , and  $\theta_i = k\pi/12$ ,  $k = 1, 3, 5$ .

### III. FULL WAVE ANALYSIS: RESULTS

A full-wave (Floquet mode) analysis (which is omitted here for brevity, and will be found in a forthcoming paper) suggests that in the limit of increasingly *large*  $a/\lambda_0$ ,  $\lambda_0$  being the field wavelength in vacuum both the internal ( $z \leq 0$ ) and the external ( $z > 0$ ) fields eventually comply with Berry's conjecture [9].

This is illustrated in Figs 7 and 8, which refer to the special (scalar) case where the electric field has only a nonzero component orthogonal to the  $xz$  plane, and all other parameters hold the same values as in Sect. 2.

The field scattered into the half-space  $z > 0$  is indeed a superposition of (propagating or evanescent) plane waves whose wave-vectors span the characteristic (grating-lobe) directions [11]

$$\sin \theta_p = \sin \theta_i - n_f \frac{p\lambda_0}{a}, \quad p \in \mathcal{Z}. \quad (3.1)$$

with (complex) amplitudes  $\Gamma_p E_i$  where  $E_i$  is the (complex) amplitude of the incident plane wave, and  $\theta_i$  is the incidence angle. It is seen from (3.1) that the number of propagating scattered plane waves is  $\propto n_f a/\lambda_0$ . Numerical simulations further show that upon increasing  $a/\lambda_0$ , the distribution of the phase among the pertinent (complex) coefficients  $\Gamma_p$  becomes more and more evenly distributed in  $(0, 2\pi)$ .

On the other hand, as seen from Fig. 7, the agreement between the (averaged [10], normalized) spatial autocorrelation function  $\langle E[\vec{r} + \hat{x}(s/2)]E^*[\vec{r} - \hat{x}(s/2)] \rangle$  of the internal ( $z \leq 0$ ) field and the  $J_0(n(z)k_0|\vec{s}|)$  Bessel function limit-form predicted by Berry's conjecture is remarkably good already at  $a/\lambda_0 = 6$ .

It is also noted that the complex coefficients  $\Gamma_p$  show a *strong* sensitivity to the incidence angle  $\theta_i$ , as illustrated in Fig. 8 for  $a/\lambda_0 = 9$ . In Fig. 8 the case of a plain sinusoidal surface is also shown ( $n_f = 1$ ), for which the  $\Gamma_p$ s are seen to depend fairly *smoothly* on the incidence angle. This peculiar behaviour has a special notable consequence, also suggested by numerical simulations. In the limit where  $a/\lambda_0 \rightarrow 0$  the spread of the distribution of field values at any given point corresponding to a large number of different incidence angles in a sector of aperture  $\Delta\theta_i$ , also remains  $\mathcal{O}(\Delta\theta_i)$ , and the mean changes with the chosen field point. On the other hand, in the opposite limit where  $a/\lambda_0 \rightarrow \infty$ , for *any* nonzero  $\Delta\theta_i$ , albeit small, the spread of the distribution *blows-up* to a finite value, while both the spread and the mean of the distribution become almost independent from the chosen field point. This scenario is likely to occur in all wave-scattering problems exhibiting chaos in the  $\lambda \rightarrow 0$  (ray) limit.

### IV. CONCLUSIONS - APPLICATION POTENTIAL

Far from being a mere exercise of pure academical interest, the proposed scattering system holds the potential for several applications of practical interest.

The findings presented above suggest that an incident narrow coherent beam of electromagnetic radiation would be scattered off the system *incoherently* and *isotropically* if  $a/\lambda_0 \gg 1$ . Thus the proposed system might be used as a *coating* for radar-puzzling applications.

The multi-hop nature of the ray-paths also suggest that upon addition of suitably *small* [12] dielectric and/or backing-surface losses the system might act as a smart radio-frequency absorber, featuring both fairly *uniform* power deposition in the dielectric bulk, and nicely small power reflection-coefficient for a *wide* interval of incidence angles.

### Acknowledgements

We acknowledge several stimulating discussions with professor Leo B. Felsen (Boston University, Boston MA, USA) and professor Giorgio Franceschetti (University of Naples, IT, and UCLA, Los Angeles CA, USA). This paper is dedicated to the memory of dr. Maurizio Mangrella.

- 
- [1] Ya. G. Sinai, Russian Math. Surveys, **25**, 137 (1970).
  - [2] L.A. Bunimovich, Chaos, **1**, 187 (1991).
  - [3] C. Bercovich, U. Smilanski and G.P. Farmelo, Eur. J. Phys., **12**, 122 (1991).
  - [4] H.J Stockmann, *Quantum Chaos: an Introduction*, Cambridge University Press, Cambridge UK (1999).
  - [5] M.V. Berry, Proc. Roy Soc. London, **A413**, 183 (1987).
  - [6] G. Veble, U. Kuhl, M. Robnik, H.J. Steckmann, J. Liu and M. Barth, Prog. Theor. Phys. Suppl. **139**, 283 (2000).
  - [7] T. Kottos, U. Smilansky, J. Fortuny and G. Nesti, Radio Science, **34** 747, (1999).
  - [8] See, e.g., A.J. Lichtenberg and M.A. Liebermann, *Regular and Stochastic Motion*, Springer Verlag, NY (1983).
  - [9] M.V. Berry, J. Phys. **A10**, 2083 (1977).
  - [10] The average is taken over several (local) wavelengths - see, e.g., [9].
  - [11] P. Beckmann and A. Spizzichino, *The Scattering of Electromagnetic Waves from Rough Surfaces*, Pergamon Press, NY (1963), ch. 4.
  - [12] The best performance is obtained when the losses are small enough to allow the existence of sufficiently long multi-hop ray-paths.

## Captions to the Figures

Fig. 1 - Sketch of problem's geometry. A perfectly conducting undulated surface with peak-to-peak height  $\Delta$  and spatial period  $a$  is topped by a dielectric layer with maximum thickness  $h$ . The refractive index of the layer matches that of the vacuum at  $z = 0$  and grows exponentially with depth up to a value  $n_f$  at  $z = -h$ .

Fig. 2 - Multi-hop ray-paths originating from close-by incidence points display rapidly increasing separations, and eventually emerge with widely different exit angles.

Fig. 3 - Exit angle (deg.) vs. scaled incidence point position  $\bar{x} = x/a$  for fixed incidence angle ( $\theta_i = \pi/12$ ) and different values of  $n_f$ :  $n_f = 1.4$  (top),  $n_f = 30$  (mid),  $n_f = 90$  (bottom).

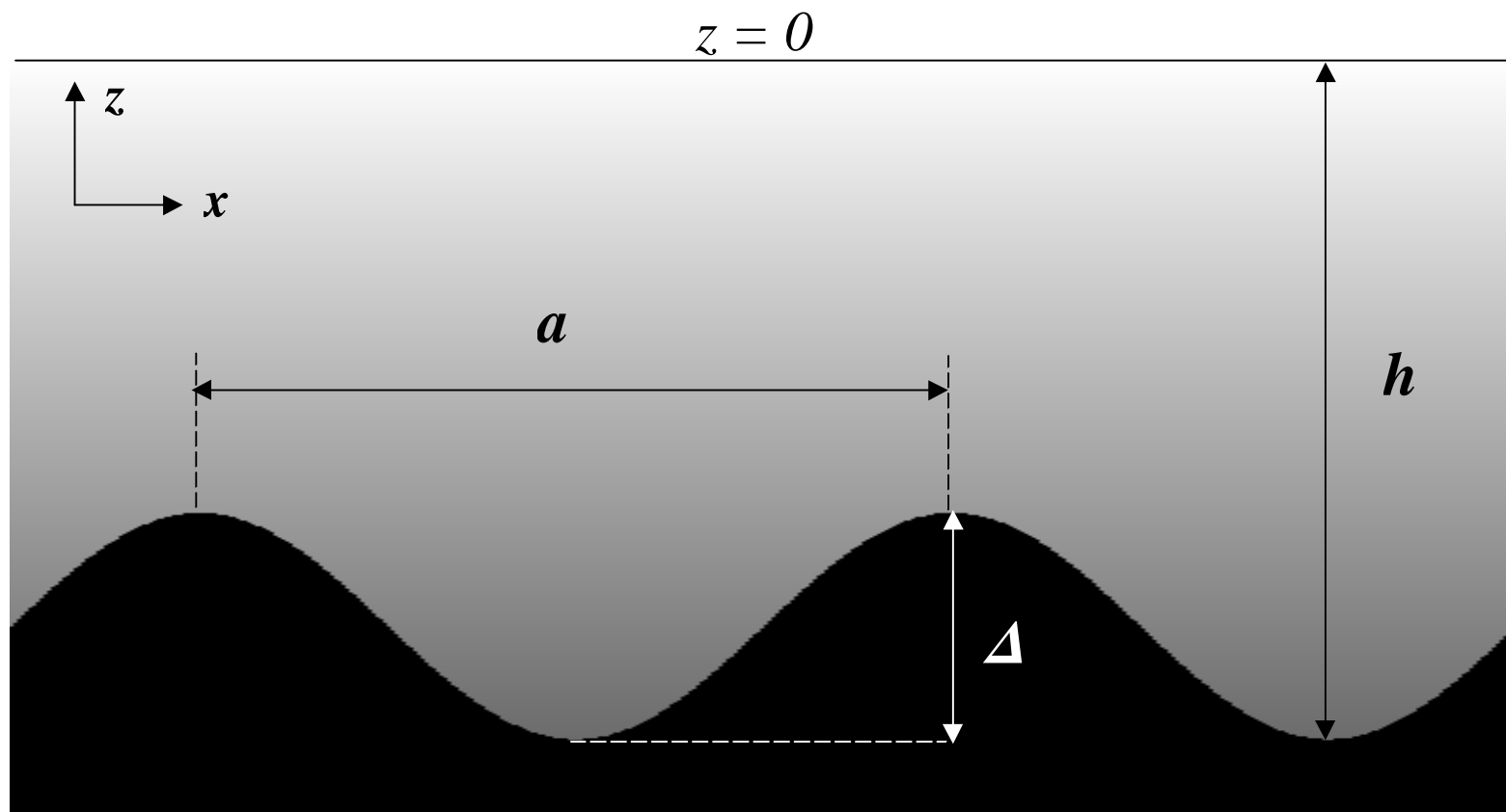
Fig. 4 - Exit angle (deg.) vs. scaled incidence point position  $\bar{x} = x/a$  for fixed  $n_f$  and different incidence angles.  $\theta_i = \pi/12$  (top),  $\theta_i = 3\pi/12$  (mid),  $\theta_i = 5\pi/12$  (bottom).

Fig. 5 - Exit angle (deg.) vs. scaled incidence point position  $\bar{x} = x/a$  for  $n_f = 15$  and  $\theta_i = \pi/12$ . Intervals corresponding to regular behaviour are observed at smaller and smaller scales (top to bottom).

Fig. 6 - Natural logarithm of separation between close-by incident rays as a function of time for  $n_f = 15$  and different incidence angles:  $\theta_i = \pi/12$  (left),  $\theta_i = 3\pi/12$  (mid),  $\theta_i = 5\pi/12$  (right).

Fig. 7 - Full wave analysis with  $a/\lambda_0 = 6$ . Averaged normalized spatial autocorrelation function of the internal ( $z \leq 0$ ) field.

Fig. 8 - Full wave analysis with  $a/\lambda_0 = 9$ . Top: modulus (left) and phase (right) of  $\Gamma_p$  for two close-by incidence angles. Bottom: the same for a plain ( $n_f = 1$ ) undulated surface.



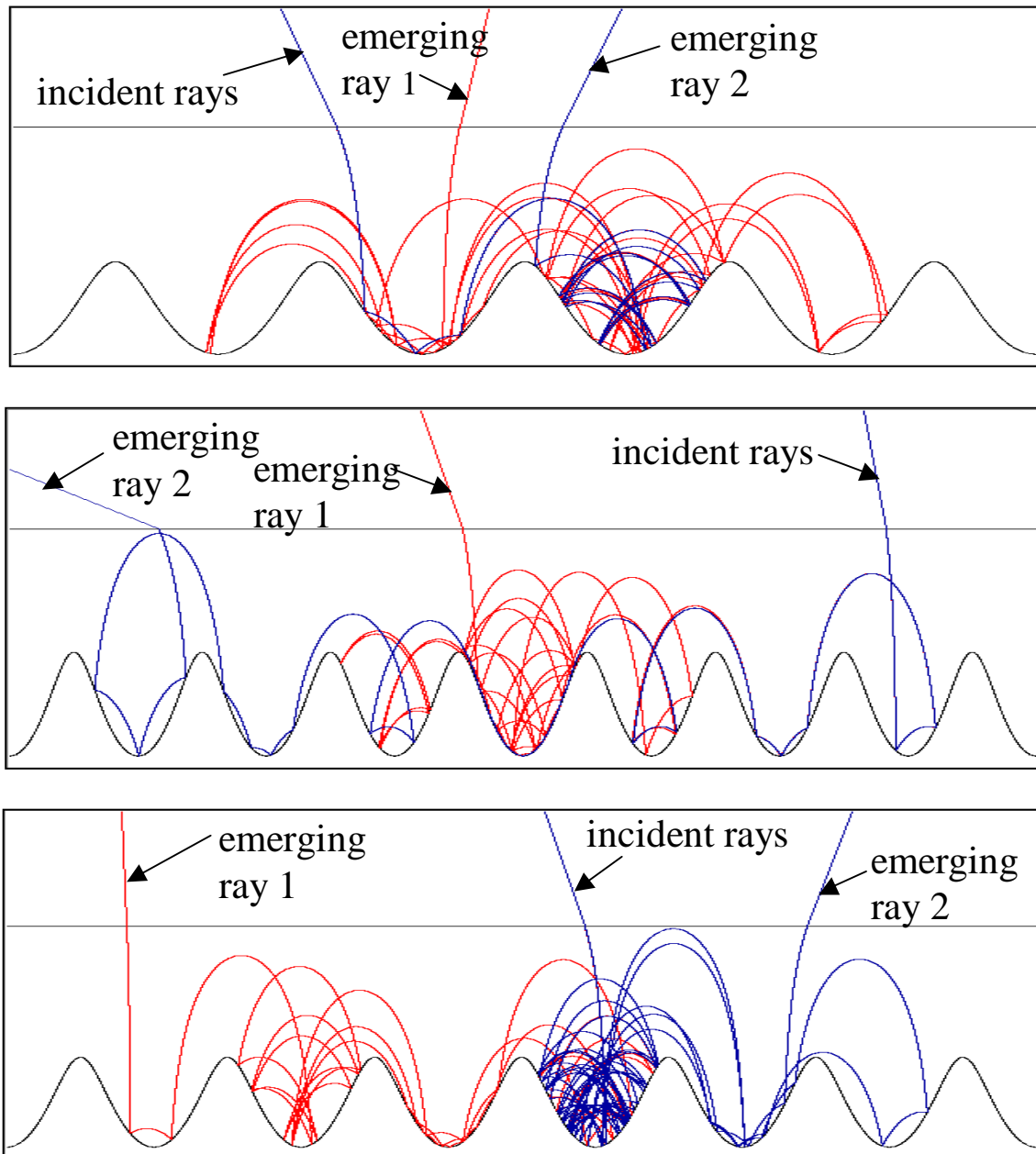


Fig.2 – Multi-hop ray-paths originating from close-by incident points.

